

Spectrally Efficient Frequency Division Multiplexing With Index-Modulated Non-Orthogonal Subcarriers

Miyu Nakao, *Student Member, IEEE*, and Shinya Sugiura, *Senior Member, IEEE*

Abstract—In this letter, we propose a novel index-modulated non-orthogonal spectrally efficient frequency-division multiplexing (SEFDM) scheme, in order to attain a higher bandwidth efficiency than the conventional orthogonal frequency-division multiplexing (OFDM) and SEFDM counterparts. More specifically, the recent index modulation concept is amalgamated with SEFDM, for the sake of reducing the effects of intercarrier interference while benefiting from SEFDM's increased spectral efficiency. We also formulate a low-complexity log-likelihood ratio (LLR)-based detection algorithm, which allows the proposed SEFDM to operate in the configuration of an arbitrarily high number of subcarriers. Our simulation results demonstrate that the proposed SEFDM scheme outperforms the conventional OFDM and SEFDM, especially in a low-rate scenario.

Index Terms—Faster-than-Nyquist, index modulation, interference, log-likelihood ratio, multicarrier, non-orthogonal subcarriers, frequency-division multiplexing.

I. INTRODUCTION

THE concept of faster-than-Nyquist (FTN) signaling has gained significant attention as a means of boosting the transmission rates of the next generation of communication systems, which is achievable without imposing additional bandwidth and power consumptions [1]–[3]. In FTN signaling, a symbol interval is set to lower than the one given by the first Nyquist criterion that guarantees the orthogonality of time-domain symbols, and hence the rate enhancement specific to FTN signaling is attainable at the expense of introducing non-orthogonality between a block of symbols.

While FTN signaling is based on non-orthogonal symbol packing in the time domain, its frequency-domain counterpart was invented in the context of multicarrier systems [4], [5], where intercarrier interference is tolerated for boosting the bandwidth efficiency, which is referred to as spectrally efficient frequency-division multiplexing (SEFDM). Furthermore, the SEFDM scheme was applied in optical [6] and satellite communication systems [7]. Moreover, in order to exploit non-orthogonal resource packing both in the time and frequency domains, a multicarrier FTN system was developed in [8], [9]. Note that in the literature, the beneficial scenario of SEFDM over orthogonal frequency-division multiplexing (OFDM) is

typically limited to as few as tens of non-orthogonal subcarriers.

Index modulation (IM) [10] is a recent promising technique that is capable of achieving specific merits over multiplexing. The IM principle is based on the activation of a subset of multiple communication resources in the space, time, and frequency domains, where the combination of activated indices is used for conveying information bits, in addition to conventional modulated symbols. Most recently, in [11], time-domain IM is combined with FTN signaling, where a high sparsity of IM symbols allows us to reduce the effects of FTN-specific ISI while benefiting from the FTN-specific increased bandwidth efficiency. Furthermore, in [12], a low-complexity successive detection algorithm based on minimum mean-square error (MMSE) criterion and log-likelihood ratio (LLR) detection was proposed for index-modulated FTN signaling. In addition, an IM scheme operating in the frequency domain, i.e., subcarrier index modulation (SIM), was developed for improving the achievable performance of OFDM [13], while in [14] multiple-mode index modulation was also applied to SIM.

Against the above-mentioned background, the novel contributions of this letter are as follows. We are the first to propose an improved SEFDM scheme where the non-orthogonal subcarriers are index-modulated for the sake of reducing the effects of detrimental intercarrier interference while benefiting from the SEFDM-specific increased bandwidth efficiency. Furthermore, we derive a low-complexity successive detection algorithm of MMSE filtering and LLR-based IM detection, which allows us to operate the proposed scheme in a scenario of a practically high number of subcarriers. Our simulation results demonstrate the fundamental benefits of the proposed SEFDM with IM (SEFDM-IM) scheme over the conventional OFDM and SEFDM schemes.

II. SYSTEM MODEL

A. Transmitted Signal Model

In the proposed SEFDM-IM scheme, N subcarriers are divided into L groups, each containing M subcarriers, and hence we have the relationship of $N = LM$. The entire frequency-domain transmission frame $\mathbf{s} \in \mathbb{C}^N$ is formulated as

$$\mathbf{s} = [s_0, s_1, \dots, s_{N-1}]^T \quad (1)$$

$$= [\mathbf{s}^{(0)T}, \mathbf{s}^{(1)T}, \dots, \mathbf{s}^{(L-1)T}]^T, \quad (2)$$

where we have the frequency-domain symbols in the l th subcarrier group as follows: $\mathbf{s}^{(l)} = [s_0^{(l)}, s_1^{(l)}, \dots, s_{M-1}^{(l)}]^T \in \mathbb{C}^M$. In this letter, we assume an additive white Gaussian noise

© 2018 IEEE. Personal use of this material is permitted. Permission from IEEE must be obtained for all other uses, in any current or future media, including reprinting/republishing this material for advertising or promotional purposes, creating new collective works, for resale or redistribution to servers or lists, or reuse of any copyrighted component of this work in other works.

M. Nakao is with the Department of Computer and Information Sciences, Tokyo University of Agriculture and Technology, Koganei, Tokyo 184-8588, Japan. S. Sugiura is with the Institute of Industrial Science, University of Tokyo, Meguro-ku, Tokyo 153-8505, Japan (e-mail: sugiura@ieee.org). (Corresponding author: Shinya Sugiura.) The present study was supported in part by the Japan Society for the Promotion of Science (JSPS) KAKENHI Grant Numbers 16KK0120, 17H03259, and 17K18871.

(AWGN) channel, for the sake of simplicity. However, the proposed scheme may be readily applicable to an arbitrary channel.

At the transmitter, B information bits $\mathbf{B} \in \mathbb{Z}^B$ are divided into L groups, each containing $b = b_1 + b_2$ bits; hence, the relationship $B = bL$ holds. The b information bits $\mathbf{b}^{(l)} \in \mathbb{Z}^b$ in the l th group are modulated onto M symbols $\mathbf{s}^{(l)}$. More specifically, the first b_1 bits out of the b information bits are used for selecting the K out of M symbols, and then the selected K symbols are modulated onto \mathcal{P} -point amplitude and phase shift keying (APSK) symbols based on b_2 bits. The remaining $M - K$ symbols are set to zero. Therefore, we have $b_1 = \lfloor \log_2 \binom{M}{K} \rfloor$ and $b_2 = K \log_2 \mathcal{P}$. Finally, in order to maintain the average transmission power per symbol at unity, the K non-zero symbols are scaled by a factor of $\sqrt{M/K}$.

Each subcarrier of the conventional SEFDM and the proposed SEFDM-IM systems is allocated in a non-orthogonal manner, such that its separation in the frequency domain is smaller than that of the OFDM counterpart, in order to increase the bandwidth efficiency. More specifically, the bandwidth compression factor is represented by $\alpha = \Delta f T$ ($\alpha < 1$), where Δf is the minimum separation in the frequency domain between the subcarriers, and T is the symbol duration in the time domain. Note that the parameter α becomes unity in the conventional OFDM system.

Hence, the transmission rate of the proposed SEFDM-IM scheme R [bps/Hz] is formulated as $R = (1/\alpha)(\lfloor \log_2 \binom{M}{K} \rfloor + K \log_2 \mathcal{P})/M$, where the coefficient $1/\alpha$ corresponds to the effects of subcarrier packing in the frequency domain, while $\lfloor \log_2 \binom{M}{K} \rfloor$ and $K \log_2 \mathcal{P}$ are the information bits carried by the IM and the conventional APSK symbols, respectively.¹

The time-domain signal representation of the proposed SEFDM-IM scheme, which is transmitted to the receiver, is given by

$$x(t) = \frac{1}{\sqrt{T}} \sum_{n=0}^{N-1} s_n \exp(j2\pi n\alpha t/T). \quad (3)$$

B. Received Signal Model

The time-domain received signals $y(t)$ are expressed as

$$y(t) = x(t) + n(t), \quad (4)$$

where $n(t)$ is the related AWGN component, which follows the complex-valued Gaussian distribution $\mathcal{CN}(0, N_0)$, N_0 being the noise variance.

The receiver consists of N correlators and a detector. In order to eliminate the effects of colored noise, an orthonormalization operation is required at each correlator. More specifically, the output of the n th receiver correlator is given by

$$r_n = \int_0^T y(t) b_n^*(t) dt \quad (n = 0, \dots, N-1), \quad (5)$$

¹Note that in the SEFDM and SEFDM-IM schemes, although the transmission rate increases with the decrease of the α value, the resultant error-rate performance typically deteriorates, due to the effects of increased inter-carrier interference.

where $b_n(t)$ is the n th orthonormal basis calculated based on the Gram–Schmidt orthonormalization method [4].

Finally, the observation statistics $\mathbf{r} = [r_0, \dots, r_{N-1}]$ can be reformulated as

$$\mathbf{r} = \mathbf{M}\mathbf{s} + \mathbf{n}, \quad (6)$$

where \mathbf{M} is the $N \times N$ covariance matrix, whose p th-row and q th-column element is calculated by

$$m_{p,q} = \frac{1}{\sqrt{T}} \int_0^T \exp(j2\pi q\alpha t/T) b_p^*(t) dt. \quad (7)$$

Furthermore, $\mathbf{n} = [n_0, \dots, n_{N-1}]$ is the related noise matrix, which is represented by

$$n_i = \frac{1}{\sqrt{T}} \int_0^T n(t) b_i^*(t) dt, \quad (8)$$

noting that the elements of \mathbf{n} remains uncorrelated with each other.

C. Error-Rate Bound

In this section, we derive the analytical BER bound of the proposed SEFDM-IM scheme, employing the optimal ML detector. The conditional pairwise error probability, where the symbol vector \mathbf{s} is misdemodulated as \mathbf{s}' , is given by [12]

$$\Pr(\mathbf{s} \rightarrow \mathbf{s}') = Q \left(\sqrt{\frac{\|\mathbf{M}(\mathbf{s} - \mathbf{s}')\|_F^2}{2N_0}} \right) \quad (9)$$

where $Q(\cdot)$ is the Q-function. The analytical BER bound is evaluated by

$$P_{\text{BER}} \leq \frac{1}{B \cdot 2^B} \sum_{\mathbf{s}} \sum_{\mathbf{s}'} d(\mathbf{s}, \mathbf{s}') \Pr(\mathbf{s} \rightarrow \mathbf{s}') \quad (10)$$

where $d(\mathbf{s}, \mathbf{s}')$ represents the Hamming distance between the binary version of \mathbf{s} and \mathbf{s}' .

III. DETECTION ALGORITHMS

A. Conventional ML Detection

The information bits estimated by the optimal maximum likelihood (ML) detection are described as

$$\hat{\mathbf{B}}_{ML} = \arg \min_{\mathbf{B}} \left\{ \|\mathbf{r} - \mathbf{M}\mathbf{B}\|^2 \right\}, \quad (11)$$

where $\|\cdot\|$ denotes the Euclidean norm. Although ML detection exhibits the attainable performance, the complexity of ML detection grows exponentially with a linear increase in the number of subcarriers N . This implies that only a limited number of subcarriers N are tractable in the conventional ML detection.

B. Conventional Successive MMSE and ML Detection

In order to reduce the high complexity, which is excessive in the above-mentioned ML detection, we revisit successive detection, based on linear MMSE, which is followed by ML detection. More specifically, the symbols are first estimated by the MMSE criterion, according to [15], [16]

$$\hat{\mathbf{s}}_{\text{MMSE}} = \frac{\mathbf{M}^H}{M/K} \left(\frac{\mathbf{M}\mathbf{M}^H}{M/K} + N_0\mathbf{I} \right)^{-1} \mathbf{r}, \quad (12)$$

where \mathbf{I} is the identity matrix.

Then, the information bits modulated on the l th subframe are detected, based on an exhaustive ML search as follows:

$$\hat{\mathbf{b}}_{\text{MMSE-ML}}^{(l)} = \arg \min_{\mathbf{b}^{(l)}} \left\{ \left\| \hat{\mathbf{s}}_{\text{MMSE}}^{(l)} - \mathbf{s}^{(l)} \right\|^2 \right\}, \quad (13)$$

where $\hat{\mathbf{s}}_{\text{MMSE}}^{(l)}$ is the l th subframe of MMSE-filtered symbols $\hat{\mathbf{s}}_{\text{MMSE}} = [\hat{\mathbf{s}}_{\text{MMSE}}^{(0)}, \dots, \hat{\mathbf{s}}_{\text{MMSE}}^{(L-1)}]^T$. While the complexity of the MMSE operation in (12) is $\mathcal{O}(N^3)$, that of the ML-based bit estimation in (13) is $\mathcal{O}(2^b)$. Hence, the total complexity imposed by detection of the whole frame does not exponentially increase with a linear increase in the number of subcarriers N , unlike the ML detection of Section III-A. Note that the original MMSE-based SEFDM symbol detection of [15] is not followed by subframe-based bit detection of (13), but by symbol-by-symbol bit detection, since the conventional SEFDM scheme, rather than the proposed SEFDM-IM scheme, was considered in [15].

C. Proposed Successive MMSE and LLR Detection

In order to further reduce the complexity associated with the ML-based bit estimation of (13), the concept of LLR detection, which was originally developed for the OFDM-IM [17] and SC-IM schemes [12], is exploited. More specifically, the LLR value of the m th symbol in the l th subframe is calculated, based on Bayes' formula, as

$$\begin{aligned} \gamma_m^{(l)} &= \ln \frac{\sum_{i=0}^{\mathcal{P}-1} P(s_m^{(l)} = \mathcal{S}_i | \hat{s}_m^{(l)})}{P(s_m^{(l)} = 0 | \hat{s}_m^{(l)})} \\ &= \ln \left(\frac{K}{M-K} \right) + \frac{|s_m^{(l)}|^2}{N_0} \\ &\quad + \ln \left(\sum_{i=0}^{\mathcal{P}-1} \exp \left(-\frac{1}{N_0} |s_m^{(l)} - \mathcal{S}_i|^2 \right) \right), \end{aligned} \quad (14)$$

where \mathcal{S}_i is the i th symbol of an \mathcal{P} -sized APSK constellation. The complexity imposed by the LLR detector of (15) is $\mathcal{O}(M)$, noting that although it is possible to directly calculate the LLR values from \mathbf{r} , this imposes an excessively high complexity, especially when the block size N is high. As mentioned in [17], in order to prevent numerical overflow, the Jacobian logarithm is typically used in (15).

Having obtained the LLR value of $\gamma_m^{(l)}$, the receiver estimates the K indices corresponding to the activated subcarriers, which are those having the K highest LLR values. Then, K APSK symbols of the K estimated active subcarriers are separately demodulated, based on a low-complexity single-subcarrier-based ML search.

D. Improved Successive MMSE and LLR Detection

The successive detection presented in Section III-B suffers from an unignorable performance penalty in comparison to the optimal ML detection. This is because the linear MMSE operation of (12) is suboptimal, while the LLR detection using (15) does not have any substantial performance loss. In order to eliminate the performance penalty imposed by

MMSE filtering, we propose improved successive MMSE and LLR detection, where we consider an increased number of candidates when estimating the active subcarriers at the stage of the LLR detection of Section III-C. This also results in an increase in the search space of the activated APSK symbols, in comparison to that of Section III-B. For the sake of simplicity, we only consider the scenario in which $K = 1$ subcarrier out of $N = M$ subcarriers is activated. However, the method can be readily extended to the generalized scenario with arbitrary parameters (K, M, N) . To be more specific, instead of selecting only the single subcarrier corresponding to the highest LLR value as in Section III-C, we here use also one additional subcarrier, the one having the second highest LLR value. Then, the search space of low-complexity single-subcarrier-based ML detection becomes doubled, in comparison to that of Section III-C. The additional computational cost of this detector over that of Section of III-C is $\mathcal{O}(LM^2)$ per block.

IV. PERFORMANCE RESULTS

In this section, we provide our simulation results, in order to characterize the achievable performance of the proposed SEFDM-IM scheme. The achievable BERs were calculated, based on Monte Carlo simulations. We employed the SEFDM-IM parameters $(M, K, \mathcal{P}) = (4, 1, 4)$.² Furthermore, the conventional SEFDM and OFDM schemes were considered as the benchmark schemes.

Fig. 1 shows the effects of bandwidth compression factor α on the achievable BER performance in the conventional SEFDM and the proposed SEFDM-IM schemes. The number of subcarriers was set as $N = 4$, and we considered an E_b/N_0 of 5 dB. The BERs of both the ML and MMSE detectors were plotted for the conventional SEFDM scheme, while all four of the detectors presented in Section III, i.e., the conventional ML, the conventional successive MMSE ML, the proposed successive MMSE-LLR, and the improved successive MMSE-LLR detectors, were compared for the proposed SEFDM-IM scheme. Observe in Fig. 1 that among the four curves associated with the proposed SEFDM-IM scheme, the proposed improved successive MMSE-LLR detector exhibited the performance close to the optimal ML detector, while accomplishing a significantly lower detection complexity than that of ML detection. Furthermore, it was found that the proposed successive MMSE-LLR detector exhibited nearly the same BER performance as the conventional successive MMSE-ML detector, which implies that introducing the LLR concept did not impose any substantial performance penalty. In addition, in Fig. 1, we see that the proposed SEFDM-IM scheme exhibits a clear performance gain over the conventional SEFDM scheme in the range of $\alpha \geq 0.7$.³

²In our extensive simulations, it was found that the SEFDM and the SEFDM-IM schemes typically exhibit the performance advantage over the OFDM counterpart for low-rate and low- K scenarios. Hence, we focused our attention only on a $K = 1$ scenario in this letter.

³In order to elaborate a little further, we further compared the minimum Euclidean distances (MEDs) between the proposed SEFDM-IM scheme and the conventional SEFDM scheme, where the SEFDM-IM scheme exhibited a higher MED than the SEFDM scheme in the range of $\alpha \geq 0.6$ for the same system parameters considered in Fig. 1.

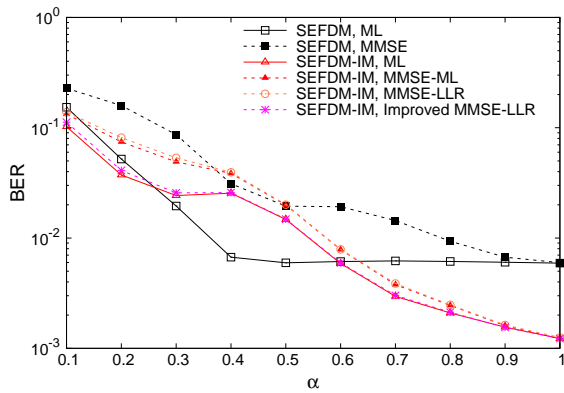


Fig. 1. Achievable BER performance of the conventional SEFDM and the proposed SEFDM-IM schemes in an AWGN channel. The number of subcarriers was set as $N = 4$, and the SEFDM-IM parameters were set as $(M, K, \mathcal{P}) = (4, 1, 4)$, while BPSK modulation was used for the conventional SEFDM scheme. E_b/N_0 was set as 5 dB.

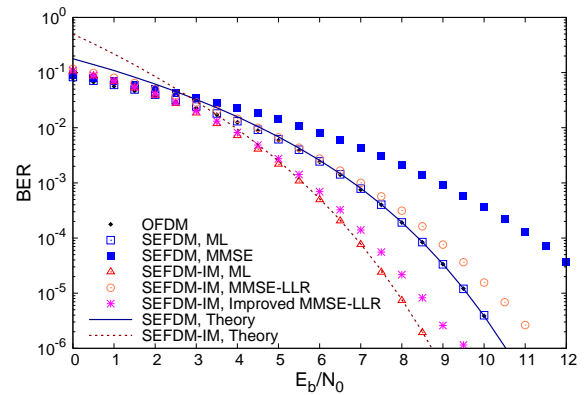


Fig. 2. Achievable BER performances of the OFDM, conventional SEFDM, and proposed SEFDM-IM schemes. The number of subcarriers was set as $N = 8$, and the SEFDM-IM parameters were set as $(M, K, \mathcal{P}) = (4, 1, 4)$. In addition, BPSK modulation was used for the OFDM and conventional SEFDM schemes.

Next, Fig. 2 compares the achievable BER performances of the OFDM, the conventional SEFDM, and the proposed SEFDM-IM schemes. Here, the number of subcarriers was set as $N = 8$, and the bandwidth compression factor was set as $\alpha = 0.8$. The optimal ML and MMSE detectors were considered for the conventional SEFDM scheme, while the optimal ML, proposed successive MMSE-LLR, and proposed successive MMSE-LLR detectors were compared for the proposed SEFDM-IM scheme. The analytical bounds of (10) were plotted for the SEFDM-IM and SEFDM schemes, while the optimal ML detection was used for the OFDM scheme. As seen from Fig. 2, regardless of the detection algorithm considered, the proposed SEFDM-IM scheme outperformed the conventional OFDM and SEFDM schemes, in this specific low-rate scenario. More specifically, the proposed SEFDM-IM employing the improved successive MMSE-LLR detector exhibited an approximately 1-dB performance gain over the OFDM and the SEFDM schemes, while the proposed SEFDM-IM scheme achieved 20% higher bandwidth efficiency than the OFDM and the SEFDM schemes.⁴

V. CONCLUSIONS

The present letter proposed a novel combination of SEFDM and IM schemes, which is capable of reducing the detrimental effects of intercarrier interference, hence allowing us to operate in a high- N scenario. Low-complexity successive detection was presented for the proposed SEFDM-IM scheme. It was demonstrated that our proposed SEFDM-IM scheme outperforms the existing OFDM and SEFDM schemes in specific low-rate scenarios.

REFERENCES

[1] J. Salz, "Optimum mean-square decision feedback equalization," *Bell System Technical Journal*, vol. 52, no. 8, pp. 1341–1373, 1973.

⁴Furthermore, we carried out additional performance comparisons for the scenario of the frequency-selective Rayleigh fading channel, where the proposed SEFDM-IM scheme still exhibited the performance advantage over the conventional SEFDM and OFDM benchmark schemes when considering the same system parameters as those used in Fig. 2.

[2] J. Mazo, "Faster-than-Nyquist signaling," *Bell System Technical Journal*, vol. 54, no. 8, pp. 1451–1462, 1975.

[3] J. Anderson, F. Rusek, and V. Owall, "Faster-than-Nyquist signaling," *Proceedings of the IEEE*, vol. 101, no. 8, pp. 1817–1830, Aug. 2013.

[4] M. Rodrigues and I. Darwazeh, "A spectrally efficient frequency division multiplexing based communications system," in *Proc. 8th International OFDM Workshop*, Hamburg, Germany, Sept. 2003, pp. 48–49.

[5] P. N. Whatmough, M. R. Perrett, S. Isam, and I. Darwazeh, "VLSI architecture for a reconfigurable spectrally efficient FDM baseband transmitter," *IEEE Transactions on Circuits and Systems I: Regular Papers*, vol. 59, no. 5, pp. 1107–1118, May 2012.

[6] I. Darwazeh, T. Xu, T. Gui, Y. Bao, and Z. Li, "Optical SEFDM system; bandwidth saving using non-orthogonal sub-carriers," *IEEE Photonics Technology Letters*, vol. 26, no. 4, pp. 352–355, Feb. 2014.

[7] H. Ghannam and I. Darwazeh, "SEFDM over satellite systems with advanced interference cancellation," *IET Communications*, vol. 12, pp. 59–66, Jan. 2018.

[8] A. Barbieri, D. Fertonani, and G. Colavolpe, "Time-frequency packing for linear modulations: spectral efficiency and practical detection schemes," *IEEE Transactions on Communications*, vol. 57, no. 10, pp. 2951–2959, Oct. 2009.

[9] D. Dasalukunte, F. Rusek, and V. Owall, "Multicarrier faster-than-Nyquist transceivers: Hardware architecture and performance analysis," *IEEE Transactions on Circuits and Systems I: Regular Papers*, vol. 58, no. 4, pp. 827–838, Apr. 2011.

[10] S. Sugiura, T. Ishihara, and M. Nakao, "State-of-the-art design of index modulation in the space, time, and frequency domains: Benefits and fundamental limitations," *IEEE Access*, vol. 5, pp. 21 774–21 790, 2017.

[11] T. Ishihara and S. Sugiura, "Faster-than-Nyquist signaling with index modulation," *IEEE Wireless Communications Letters*, vol. 6, no. 5, pp. 630–633, Oct. 2017.

[12] M. Nakao, T. Ishihara, and S. Sugiura, "Dual-mode time-domain index modulation for nyquist-criterion and faster-than-nyquist single-carrier transmissions," *IEEE Access*, vol. 5, pp. 27 659–27 667, 2017.

[13] N. Ishikawa, S. Sugiura, and L. Hanzo, "Subcarrier-index modulation aided OFDM - will it work?" *IEEE Access*, vol. 4, pp. 2580–2593, 2016.

[14] M. Wen, E. Basar, Q. Li, B. Zheng, and M. Zhang, "Multiple-mode orthogonal frequency division multiplexing with index modulation," *IEEE Transactions on Communications*, vol. 65, no. 9, pp. 3892–3906, Sept. 2017.

[15] I. Kanaras, A. Chorti, M. R. D. Rodrigues, and I. Darwazeh, "A combined MMSE-ML detection for a spectrally efficient non orthogonal fdm signal," in *5th International Conference on Broadband Communications, Networks and Systems*, 2008, pp. 421–425.

[16] S. Sugiura and L. Hanzo, "Single-RF spatial modulation requires single-carrier transmission: Frequency-domain turbo equalization for dispersive channels," *IEEE Transactions on Vehicular Technology*, vol. 64, no. 10, pp. 4870–4875, Oct. 2015.

[17] E. Başar, Ü. Aygölü, E. Panayırçı, and H. V. Poor, "Orthogonal frequency division multiplexing with index modulation," *IEEE Transactions on Signal Processing*, vol. 61, no. 22, pp. 5536–5549, Nov. 2013.